The Cryosphere Discuss., 4, 2593–2613, 2010
www.the-cryosphere-discuss.net/4/2593/2010/
doi:10.5194/tcd-4-2593-2010

The Cryosphere Discussions

Longest time series of glacier mass changes in the Himalaya based on stereo imagery

T. Bolch[1,3], T. Pieczonka[1], and D. I. Benn[2,4]

[1]Institut für Kartographie, Technische Universität Dresden, Germany
[2]The University Centre in Svalbard, Norway
[3]Geographisches Institut, Universität Zürich, Switzerland
[4]University of St Andrews, UK

Received: 1 December 2010 – Accepted: 9 December 2010 – Published: 20 December 2010

Correspondence to: T. Bolch (tobias.bolch@geo.uzh.ch)

Published by Copernicus Publications on behalf of the European Geosciences Union.

Abstract

Mass loss of Himalayan glaciers has wide-ranging consequences such as declining water resources, sea level rise and an increasing risk of glacial lake outburst floods (GLOFs). The assessment of the regional and global impact of glacier changes in the Himalaya is, however, hampered by a lack of mass balance data for most of the range. Multi-temporal digital terrain models (DTMs) allow glacier mass balance to be calculated since the availability of stereo imagery. Here we present the longest time series of mass changes in the Himalaya and show the high value of early stereo spy imagery such as Corona (years 1962 and 1970) aerial images and recent high resolution satellite data (Cartosat-1) to calculate a time series of glacier changes south of Mt. Everest, Nepal. We reveal that the glaciers are significantly losing mass with an increasing rate since at least ∼1970, despite thick debris cover. The specific mass loss is $0.32 \pm 0.08\,\mathrm{m\,w.e.\,a^{-1}}$, however, not higher than the global average. The spatial patterns of surface lowering can be explained by variations in debris-cover thickness, glacier velocity, and ice melt due to exposed ice cliffs and ponds.

1 Introduction

Recent debate on whether Himalayan glaciers are shrinking faster than in other parts of the world (Cogley et al., 2010) highlighted the lack of knowledge about the glaciers in this region. Glacier mass balance is the variable which can be directly linked to climate and that can be compared to other regions. However, only a few in-situ mass balance measurements have been made on Himalayan glaciers, and existing data series are short (Kulkarni, 1992; Fujita et al., 2001; Wagnon et al., 2007; Dobhal et al., 2008). Comparisons of digital terrain models for different years can complement field measurements, and allow regional mass balance to be estimated (Bamber and Rivera, 2007). However, to date it has only been applied to some glaciers in Western Himalaya for 1999 to 2004 (Berthier et al., 2007) and for four glaciers at Mt. Everest for 1962 to

TCD
4, 2593–2613, 2010

2002 (Bolch et al., 2008b). Broader and more detailed knowledge of glacier mass balance are also needed to decrease the high uncertainty about the importance of Himalayan glaciers for water resources (e.g., Immerzeel et al., 2010) and sea level rise (e.g., Braithwaite and Raper, 2002). Finally, improved knowledge of glacier recession is needed to better estimate risk of GLOFs (Richardson and Reynolds, 2000).

The aim of this study is first to evaluate the results of the pilot study by Bolch et al. (2008b) by independent data sets. This study revealed surface lowering by analysing a 1962 Corona (year 1962) and an ASTER DTM (mean year 2002) but had high uncertainties. The second aim is to present mass balance estimates for larger sample of glaciers around Mt. Everest including Imja Glacier which is of high interest due to the proglacial lake which formed in the 1960s (Bolch et al., 2008a; Fujita et al., 2009). In addition, the mass balance of the entire Khumbu Glacier will be presented for the first time. Thirdly, we aim to produce the first time-series of mass changes at Mt. Everest, Nepal to show the suitability of different optical imagery to derive mass balance variability over time and to discuss the possible causes of the surface changes.

The tongues of nine studied glaciers are heavily covered by supraglacial debris (Fig. 1), with average debris thickness increasing downglacier (Nakawo et al., 1999; Hambrey et al., 2008). The glaciers are mainly nourished by snow and ice avalanches which accumulate cones below the steep headwalls. Only Khumbu Glacier has an extensive accumulation area (Western Cwm). Glacier equilibrium line altitudes (ELAs) are roughly estimated to be situated above 5600 m (Asahi, 2001). Ice velocities typically decrease downglacier from the ELA with extensive stagnant ice in their lower reaches (Bolch et al., 2008a; Quincey et al., 2009). Between 1962 and 2005 the overall glacier area loss in the study area was ~5% with an increasing debris-covered area but an almost stable terminus positions (Bolch et al., 2008b).

TCD
4, 2593–2613, 2010

2 Data and methodology

We used 1970 Corona KH-4B (declassified US spy imagery) data, 1984 aerial photographs (camera: Wild RC 10) (Altherr and Grün, 1990) and 2007 Cartosat-1 (Indian Remote Sensing Satellite, IRS P5) images (Table 1). In addition, we used previously generated 1962 Corona and 2002 ASTER DTMs (Bolch et al., 2008b). We did not consider the data from the Shuttle Radar Topography Mission (SRTM) due to large data gaps in the area of interest and the coarser spatial resolution (90 m) in comparison to the ASTER DTM (30 m). We applied the Remote Sensing Software Package Graz (RSG) 6.13 for processing Corona, PCI Geomatica OrthoEngine 10.2 for Cartosat, and Leica Photogrammetry Suite (LPS) 9.1 for the aerial images. We used 14 non-differential GPS points acquired in 2006 and 2008 and points from the National Geographic 1:50k topographic map (Altherr and Grün, 1990) as ground control points (GCPs). The $RMSE_z$ and $RSME_{x,y}$ of the map were computed based on the GPS points to be 20.6 m and 17.8 m, respectively. This matches almost the results achieved by Altherr and Grün (1990). In addition, we used automatically selected tie points (TPs) to improve the sensor model. The overall quality of the generated raw DTMs appears promising as the glacier tongues are almost fully represented (Fig. 3). Data gaps occur mainly due to snow cover and cast shadow.

In order to address glacier elevation changes as precisely as possible it is recommended to adjust the DTMs relative to each other (Nuth and Kääb, 2010). Tilts which occurred especially in the Corona DTM were corrected using trend surfaces calculated based on manually selected points on stable extraglacial areas throughout the DTMs (Fig. 2, Pieczonka et al., 2010). We observed slight horizontal shifts of the generated DTMs although we used the same GCPs for all images whenever possible. In order to avoid biases introduced thereby and to improve the z-accuracy, we choose the Cartosat-1 DTM as the master reference as it has a high spatial resolution and showed the lowest mean elevation difference (5.9 m) and $RMSE_z$ (19.2 m) relative to the SRTM3 DTM. We co-registered the other DTMs to it by minimizing the standard

TCD
4, 2593–2613, 2010

deviation of the elevation differences (Berthier et al., 2007). The applied shifts varied between 5 and 30 m. Altitudinal differences which exceeded ± 100 m (usually around data gaps and near DTM edges) were omitted assuming that these values represent outliers similar to the assumptions of Berthier et al. (2010). We resampled all DTMs bilinearly to the pixel size of the coarsest DTM (30 m) in order to reduce the effect of different resolutions.

The uncertainties of the DTMs were calculated based on more than 200 height points on stable areas relative to the 2007 master DTM. The mean difference between the final adjusted DTMs was in the range −0.1 to −1.8 m while the RMSE_z was 7.8 to 19.8 m (Table 1). To address the uncertainty of the elevation differences of the glaciated areas we calculated statistical parameters for the differences of ice covered and the non-ice covered areas separately (Table 2). The standard deviation (STDV) of the non glacier area or the RSME_z can be used as a first estimate of the uncertainty, but would probably overestimate it (Berthier et al., 2007). We used the standard error (SE) and the mean elevation difference (MED) of the non glacier area as an estimate of the uncertainty according to the law of error propagation:

$$e = \sqrt{\mathrm{SE}^2 + \mathrm{MED}^2}$$

while we account only each 20th pixel as suggested by Koblet et al. (2010) to minimize the effect of auto-correlation.

Volume change was calculated for each glacier assuming that the density profile remains unchanged and that only ice is lost or gained (Paterson, 1994; Zemp et al., 2010). To convert volume changes into mass change, we assumed an ice density of 900 kg m^{-3} and assigned an additional uncertainty of 7% due to lack of ground truth (Zemp et al., 2010). We interpolated small data voids (<10 pixel) within the ice covered areas using a spline algorithm. We did not fill the larger data gaps e.g. on steep slopes. The glacier tongues, the avalanche cones and Western Cwm are represented in the DTMs of 1970, 2002, and 2007 (Fig. 3, Tables 3, 4) which allow estimation of the mass balance for the entire glacier. Only Changri Nup, Duwo, and the debris-free Chukhung

Glacier have large data gaps. Detailed investigations on Khumbu Glacier are limited to the tongue below ∼5700 m (mainly the ablation area) due to the small coverage of the aerial images.

3 Volume changes and mass losses

3.1 Periods 1970–2007 and 2002–2007 for the whole study area

Between 1970 and 2007 significant surface lowering occurred on all investigated glaciers (Fig. 3, Table 2). The greatest lowering was on Imja/Lhotse Shar Glacier. Except for this glacier, which displays surface lowering throughout the terminus, most glaciers show maximum lowering in their mid ablation zones, with a negligible change near their termini. Overall ice loss is estimated to be >0.6 km^3 with an average surface lowering of 0.36 ± 0.07 m a^{-1} or a specific mass balance of -0.32 ± 0.08 m w.e. a^{-1} between 1970 and 2007 (Table 3). The specific mass balance for the debris-covered parts only is -0.35 ± 0.08 m w.e. a^{-1}, clearly showing that significant mass loss occured despite thick debris-cover. Most glaciers also experienced surface lowering between 2002 and 2007 (Fig. 3, Table 3). The specific mass loss of all 10 glaciers has possibly doubled compared to 1970–2007 (-0.79 ± 0.42 m w.e. a^{-1}). However, the uncertainty is high.

3.2 Detailed investigations on Khumbu Glacier

The ablation area of Khumbu Glacier lost mass in all investigated time periods (Table 3). DTM differencing (Figs. 3 and 4) and longitudinal profiles, in particular for 1970–2007, show almost no ice loss in the clean ice zone below Khumbu Icefall (Fig. 5, Sect. A); an increasing ice loss in the debris-covered part, with the highest lowering between 2 and 8 km from the terminus (B, C), and almost no ice loss within ∼1.5 km of the terminus (D). For 1970–1984 only lowering between ∼1.5 and 5.5 km of the terminus is significant (Fig. 5). Between 1970 and 2007, average surface lowering rate in the ablation area was -0.38 ± 0.07 m a^{-1}. The rate for 1984–2002 is higher than for

1962–1970 and 1970–1984, and comparison of the recent DTMs (2002–2007) suggests further accelerated ice loss (Table 4). However, these differences are hardly statistically significant. Comparing the periods 1970–1984 and 1984–2007, however, shows a significant increase in the rate of ice loss (0.18 ± 0.30 m w.e. a^{-1} in comparison to 0.53 ± 0.15 m w.e. a^{-1}). The accumulation zone of Khumbu Glacier has possibly also lost mass during the investigated time, while there might be a slight mass gain in recent time (2002–2007).

4 Discussion

Stereo capability, acquisition in the 1960s and 1970s and relatively high spatial resolution make Corona imagery a valuable source for geodetic mass balance estimations. The generation of mass balance time series using diverse data sets with different resolution requires careful co-registration and adjustment. Although inaccuracies remain on steep slopes most of the glacier area is not affected by these biases. The quality of the DTMs is supported by the observation that the highest thinning at Khumbu Glacier between 1970 and 1984 (arrow Fig. 4) coincides with a lake which is visible on the 1984 aerial photos and drained afterwards.

The calculated average 1970–2007 thickness changes for the whole study area based on independent data sets confirms the values of calculated by Bolch et al. (2008b) for 1962–2002. The wider coverage of this study including Imja Glacier, and the accumulation area of Khumbu Glacier, as well as the multi-temporal coverage, allow greater insight into decadal glacier changes and the influence of debris cover. The longitudinal profile of glacier thinning of Khumbu Glacier shows similar characteristics to those presented by Nakawo et al. (1999) based on estimated ice flow and thermal properties derived from Landsat data. Very low slope angles in the 2007 longitudinal profile (Fig. 5b) indicate that a glacial lake could develop about 1.5 to 3 km upstream of the terminus, as predicted in simulations based on a 1D-coupled mass balance and flow model by Naito et al. (2000). These observations increase confidence in the observed patterns of down-wasting, despite the existing uncertainties.

The pattern of surface lowering on Khumbu Glacier can be explained in terms of ice dynamics and surface melt rates. Sustained high rates of ice delivery below the icefall largely offset melt in the upper ablation area, where debris cover is thin or absent (Fig. 5a, section A). Further downglacier, thin debris cover increases the ice melt (section B), in line with field measurements of increased surface lowering (Takeuchi et al., 2000). Thinning rates remain high downglacier despite an increasing debris thickness, due to very low glacier velocities and ablation associated with supraglacial lakes and exposed ice cliffs (Sakai et al., 2000, 2002) (C). Almost no thinning was observed within 1 km of the terminus (D), which may reflect either a thick, complete debris cover or indicate that ice loss is already complete. The possible slight surface lowering in the accumulation area of the glacier might be due to less snowfall. This is consistent with an ice core record at the East Rongbuk Glacier north of Mt. Everest that indicates decreasing snow accumulation for 1970–2001 (Kaspari et al., 2008). The highest mass loss of Imja Glacier can be at least partly attributed to the proglacial Imja Lake, which enhances ice losses by calving. This lake grew significantly since its formation in the late 1960s up to ~0.9 km^2 in 2008 (Fujita et al., 2009; Bolch et al., 2008a). The comparatively thin debris cover of Imja Glacier, apparent in exposed ice cliffs, and its low glacier velocity are likely to be the other reasons for the higher mass loss. Imja Glacier is the only investigated glacier where a slight thinning is also observed at the terminal moraine situated below Imja Lake. This is in line with recent field measurements in this area which revealed a lowering of about 1 m a^{-1} (Fujita et al., 2009). The mass loss of the smaller glaciers, such as Amphu Laptse Glacier, amounts to half of that of Imja Glacier but is still significant.

The studied glaciers show an accelerated ice loss since 1984 and especially for the period 2002–2007. The recent trend of more negative mass balances since 2002, however, needs further investigation, as it is only partly statistically significant. Accelerated thinning could reflect decreasing velocity (Quincey et al., 2009), higher air temperatures (Prasad et al., 2009), decreasing snow accumulation (Kaspari et al., 2008) or a combination of those.

TCD
4, 2593–2613, 2010

The specific mass loss of Khumbu Glacier for 1970–2007, at -0.27 ± 0.08 m w.e. a^{-1} is lower than that of other Himalayan glaciers including Chhota Shigri Glacier (-0.98 m w.e. a^{-1}, 2002–2006, Wagnon et al., 2007, and -1.02 to -1.12 m w.e. a^{-1}, 1999–2004, Berthier et al., 2007) or the small debris-free Glacier AX010 (-0.6 to -0.8 m w.e. a^{-1}, 1978–1999, Fujita et al., 2001) but similar to Dokriani Glacier (-0.32 m w.e. a^{-1}, 1992–2000, Dobhal et al., 2008). However, the different observation times and glacier sizes have to be considered, and Khumbu Glacier has also a more negative mass balance in recent years. The tendency towards increased mass loss has also been observed worldwide and for the few other Himalayan glaciers with mass balance estimates (Cogley, 2010). The mass loss of the investigated glaciers is similar to the average mass loss of the 30 reference glaciers worldwide for 1976–2005 (-0.32 w.e. a^{-1}) (Zemp et al., 2009).

5 Conclusions

This study presents the longest time series of geodetically derived mass-balance estimates obtained to date in the Himalaya. Geodetic mass-balance estimates based on early stereo Corona and recent satellite data are suitable for tracking glacier changes through time, thus filling major gaps in glaciological knowledge of the Himalaya and other mountain regions. However, careful adjustments relative to each DTM are necessary to obtain suitable accuracy of DTMs based on different data sources with different resolutions. Mass balance information is urgently needed to improve estimates of the response of Himalayan glaciers to climate change and predict future glacier change and its influence on water resources, river runoff, sea level rise, and glacial hazards.

Glaciers south of Mt. Everest have continuously lost mass from 1970 until 2007, with an increasing rate in recent years. All glaciers lost mass despite partly thick debris-cover. The highest loss was observed at Imja Glacier which terminates into a lake. The specific mass balance of the investigated glaciers of -0.32 ± 0.08 m w.e. a^{-1} is not higher than the global average.

Acknowledgement. We thank M. Buchroithner for the support and ICIMOD for cooperation. We are grateful for the thorough reviews of an earlier version of this manuscript. H. Raggam helped with RSG. GAF AG offered Cartosat-1 data at a reduced price. D. Quincey provided the 1984 images and DFG (Deutsche Forschungs-gemeinschaft) financial support (Code BU 949/15-1).

References

Altherr, W. and Grün, A.: Mt. Everest Karte 1:50 000 – Faszination eines Kartenprojektes, Schweizerische Zeitschrift für Vermessung, Kulturtechnik und Photogrammetrie, February, 90–97, 1990.

Asahi, K.: Inventory and recent variations of glaciers in the Eastern Nepal Himalayas, Seppyo, 159–169, 2001.

Bamber, J. L. and Rivera, A.: A review of remote sensing methods for glacier mass balance determination, Global Planet. Change, 59, 138–148, 2007.

Berthier, E., Arnaud, Y., Rajesh, K., Sarfaraz, A., Wagnon, P., and Chevallier, P.: Remote sensing estimates of glacier mass balances in the Himachal Pradesh (Western Himalaya, India), Remote Sens. Environ., 108, 327–338, 2007.

Berthier, E., Schiefer, E., Clarke, G. K. C., Menounos, B., and Rémy, F.: Contribution of Alaskan glaciers to sea-level rise derived from satellite imagery, Nat. Geosci., 3, 92–95, doi:10.1038/ngeo737, 2010.

Bolch, T., Buchroithner, M. F., Peters, J., Baessler, M., and Bajracharya, S.: Identification of glacier motion and potentially dangerous glacial lakes in the Mt. Everest region/Nepal using spaceborne imagery, Nat. Hazards Earth Syst. Sci., 8, 1329–1340, doi:10.5194/nhess-8-1329-2008, 2008a.

Bolch, T., Buchroithner, M. F., Pieczonka, T., and Kunert, A.: Planimetric and volumetric Glacier changes in Khumbu Himalaya since 1962 using Corona, Landsat TM and ASTER data, J. Glac., 54, 592–600, 2008b.

Braithwaite, R. J. and Raper, S. C. B.: Glaciers and their contribution to sea level change, Phys. Chem. Earth, 27, 1445–1454, 2002.

Cogley, J. G.: Himalayan glaciers now and in 2035, in: Encyclopaedia of Snow, Ice and Glaciers, edited by: Singh, V. P., Singh, P., and Haritashya, U. K., Springer, in press, 2010.

TCD

4, 2593–2613, 2010

Himalayan glacier mass changes

T. Bolch et al.

Cogley, J. G., Kargel, J. S., Kaser, G., and Van der Veen, C. J.: Tracking the source of glacier misinformation, Science, 327, 522, 2010.

Dobhal, D. P., Gergan, J. T., and Thayyen, R. J.: Mass balance studies of the Dokriani Glacier from 1992 to 2000, Garhwal Himalaya, India, Bull. Glaciol. Res., 25, 9–17, 2008.

Fujita, K., Kadota, T., Rana, B., Shresta, R. B., and Ageta, Y.: Shrinkage of Glacier AX010 in shorong region, Nepal Himalayas in the 1990s, Bull. Glaciol. Res., 18, 51–54, 2001.

Fujita, K., Sakai, A., Nuimura, T., Yamaguchi, S., and Sharma, R. R.: Recent changes in Imja Glacial Lake and its damming moraine in the Nepal Himalaya revealed by in situ surveys and multi-temporal ASTER imagery, Environ. Res. Lett., 4, 045205, 2009.

Hambrey, M., Quincey, D., Glasser, N. F., Reynolds, J. M., Richardson, S. J., and Clemmens, S.: Sedimentological, geomorphological and dynamic context of debris-mantled glaciers, Mount Everest (Sagarmatha) region, Nepal, Quaternary Sci. Rev., 27, 2341–2360, 2008.

Immerzeel, W. W., van Beek, L. P. H., and Bierkens, M. F. P.: Climate change will affect the Asian water towers, Science, 328, 1382–1385, 2010.

Kaspari, S., Hooke, R. L. B., Mayewski, P. A., Kang, S., Hou, S., and Qin, D.: Snow accumulation rate on Qomolangma (Mount Everest), Himalaya: synchroneity with sites across the Tibetan Plateau on 50–100 year timescales, J. Glac., 54, 343–352, 2008.

Koblet, T., Gärtner-Roer, I., Zemp, M., Jansson, P., Thee, P., Haeberli, W., and Holmlund, P.: Reanalysis of multi-temporal aerial images of Storglaciären, Sweden (1959–99) – Part 1: Determination of length, area, and volume changes, The Cryosphere, 4, 333–343, doi:10.5194/tc-4-333-2010, 2010.

Kulkarni, A. V.: Mass balance of Himalayan glaciers using AAR and ELA methods, J. Glac., 38, 101–104, 1992.

Naito, N., Nakawo, M., Kadota, T., and Raymond, C. F.: Numerical simulation of recent shrinkage of Khumbu Glacier, Nepal Himalayas, IAHS Publ., 264, 245–254, 2000.

Nakawo, M., Yabuki, H., and Sakai, A.: Characteristics of Khumbu Glacier, Nepal Himalaya: recent changes in the debris-covered area, Ann. Glac., 28, 118–122, 1999.

Nuth, C. and Kääb, A.: What's in an elevation difference? Accuracy and corrections of satellite elevation data sets for quantification of glacier changes, The Cryosphere Discuss., 4, 2013–2077, doi:10.5194/tcd-4-2013-2010, 2010.

Paterson, W. S. B.: The Physics of Glaciers, 3rd Edn., Pergamon, New York, 1994.

Pieczonka, T., Bolch, T., and Buchroithner, M. F.: Generation and evaluation of multi-temporal digital elevation models from different optical sensors, J. Photogramm. Rem. Sens., in revision, 2010.
Prasad, A. K., Yang, K.-H. S., El-Askary, H. M., and Kafatos, M.: Melting of major Glaciers in the western Himalayas: evidence of climatic changes from long term MSU derived tropospheric temperature trend (1979–2008), Ann. Geophys., 27, 4505–4519, doi:10.5194/angeo-27-4505-2009, 2009.
Quincey, D., Luckman, A., and Benn, D.: Quantification of Everest region glacier velocities between 1992 and 2002, using satellite radar interferometry and feature tracking, J. Glac., 55, 596–606, 2009.
Richardson, S. D. and Reynolds, J. M.: An overview of glacial hazards in the Himalayas, Quatern. Int., 65/66, 31–47, 2000.
Sakai, A., Takeuchi, N., Fujita, K., and Nakawo, M.: Role of supraglacial ponds in the ablation process of a debris-covered glacier in the Nepal Himalayas., IAHS Publ., 264, 119–130, 2000.
Sakai, A., Nakawo, M., and Fujita, K.: Distribution characteristics and energy balance of ice cliffs on debris-covered glaciers, Nepal Himalaya, Arct. Antarct. Alp. Res., 34, 12–19, 2002.
Takeuchi, Y., Kayastha, R. B., and Nakawo, M.: Characteristics of ablation and heat balance in debris-free and debris-covered areas on Khumbu Glacier, Nepal Himalayas, in the pre-monsoon season, IAHS Publ., 264, 53–61, 2000.
Wagnon, P., Linda, A., Arnaud, Y., Kumar, R., Sharma, P., Vincent, C., Pottakkal, J. G., Berthier, E., Ramanathan, A., Hasnain, S. I., and Chevallier, P.: Four years of mass balance on Chhota Shigri Glacier, Himachal Pradesh, India, a new benchmark glacier in the western Himalaya, J. Glac., 53, 603–611, 2007.
Zemp, M., Hoelzle, M., and Haeberli, W.: Six decades of glacier mass balance observations – a review of the worldwide monitoring network, Ann. Glac., 50, 101–111, 2009.
Zemp, M., Jansson, P., Holmlund, P., Gärtner-Roer, I., Koblet, T., Thee, P., and Haeberli, W.: Reanalysis of multi-temporal aerial images of Storglaciären, Sweden (1959–99) – Part 2: Comparison of glaciological and volumetric mass balances, The Cryosphere, 4, 345–357, doi:10.5194/tc-4-345-2010, 2010.

TCD
4, 2593–2613, 2010

Table 1. Utilized imagery and derived DTM characteristics.

Date	Sensor	Spatial resolution (m)		Vertical accuracy (m) before adjustment		Vertical accuracy (m) after adjustment	
		Imagery	Original DTM	Mean elev. diff.	$RMSE_z$	Mean elev. diff.	$RMSE_z$
1962	Corona KH-4	7.6	20	−53.0	56.9	−0.1	19.8
1970	Corona KH-4B	5.2	15	−9.0	28.6	−0.5	18.8
1984	Wild RC-10	0.5	15	8.2	11.2	−1.8	7.8
2002	ASTER	15	30	12.8	29.5	−1.5	10.1
2007	Cartosat-1	2.5	10	Reference	Reference	Reference	Reference

TCD
4, 2593–2613, 2010

Table 2. Statistics of the DTM differences for the investigated periods.

Period	DTM coverage study area (km^2)	DTM coverage glac. (km^2)	Mean elev. diff. no glac. (m)	STDV no glac. (m)	Mean elev. diff. glac. (m)	STDV glac. (m)	*N* no glac.	SE no glac. (m)
1962–1970	137.8	25.4	–0.9	22.3	–1.9	15.7	319	1.3
1970–1984	83.8	24.4	–3.6	26.3	–9.9	16.1	163	2.1
1984–2002	83.4	25.7	–2.2	26.5	–5.4	18.2	160	1.7
2002–2007	174.5	59.8	+2.1	20.9	–3.2	13.5	321	1.2
1984–2007	80.6	20.9	+2.4	15.8	–9.2	15.4	109	1.5
1970–2007	152.9	46.5	+2.2	19.4	–13.2	15.6	293	1.1

glac.: glacier area, no glac.: non glacier area, *N*: number of considered pixels

TCD
4, 2593–2613, 2010

Table 3. Glacier volume loss and mass balance 1970–2007, and 2002–2007.

Glacier	Glacier size (km^2)	Period 1970–2007: Glacier area covered by DTM (km^2)	Period 1970–2007: Average elev. diff. (m)	Period 1970–2007: Specific mass balance (m w.e. a^{-1})	Period 2002–2007: Glacier area covered by DTM (km^2)	Period 2002–2007: Average elev. diff. (m)	Period 2002–2007: Specific mass balance (m w.e. a^{-1})
Changri Shar/Nup	13.0	6.85	−11.6 ± 2.50	−0.28 ± 0.08	6.93	−1.6 ± 2.6	−0.29 ± 0.42
Khumbu accumulation area[1]	6.2	4.30	−6.2 ± 2.5	−0.17 ± 0.08	4.66	+1.2 ± 2.6	+0.22 ± 0.48
Khumbu ablation area[1]	10.8	10.0	−13.9 ± 2.5	−0.34 ± 0.08	10.1	−4.0 ± 2.6	−0.71 ± 0.42
Whole Khumbu	17.0	14.26	−11.1 ± 2.5	−0.27 ± 0.08	14.7	−2.5 ± 2.6	−0.45 ± 0.44
Nuptse	4.0	3.45	−9.4 ± 2.5	−0.25 ± 0.08	3.52	−2.2 ± 2.6	0.40 ± 0.45
Lhotse Nup	2.0	1.86	−7.6 ± 2.5	−0.18 ± 0.07	1.86	−5.7 ± 2.6	−1.03 ± 0.40
Lhotse	6.5	6.71	−10.7 ± 2.5	−0.26 ± 0.08	6.71	−6.1 ± 2.6	−1.10 ± 0.40
Lhotse Shar/ Imja[2]	10.7	8.65	−20.6 ± 2.5	−0.50 ± 0.09	8.87	−8.1 ± 2.6	−1.45 ± 0.37
Amphu Laptse	1.5	1.05	−10.0 ± 2.5	−0.24 ± 0.08	1.08	−4.3 ± 2.6	−0.77 ± 0.42
Chukhung	3.8	1.88	−5.3 ± 2.5	−0.30 ± 0.08	3.20	0 ± 2.6	0 ± 0.50
Amadablam	2.2	1.86	−12.0 ± 2.5	−0.29 ± 0.08	2.50	−3.1 ± 2.6	−0.56 ± 0.44
Duwo	1.0	0.37	−12.2 ± 2.5	−0.30 ± 0.08	0.37	−10.9 ± 2.6	−1.96 ± 0.34
Sum/Average	61.7	46.9	−13.3 ± 2.5	−0.32 ± 0.08	49.6	−4.4 ± 2.6	−0.79 ± 0.42

[1] We assumed an ELA of 5700 m based on Ashai (2001) and interpretation of the satellite images.
[2] For the year 2007, the estimated volume of Imja lake (37.8×10^6 m^3, calculated based on the area extent 0.91 km^2 and the average depth of 41.4 m) was added to the elevation difference of 1970–2007. For 2002–2007 we added the volume difference between 2007 and 2002 (2.0×10^6 m^3). Data is based on Fujita et al. (2009).

TCD
4, 2593–2613, 2010

Table 4. Volume loss/mass balance of the ablation area of Khumbu Glacier 1962–2007.

Time	DTM coverage (km^2)	Average down-wasting (m)	Specific mass balance ($m\,w.e.\,a^{-1}$)
1962–1970	4.9	-2.74 ± 1.54	-0.31 ± 0.19
1970–1984	9.9	-2.53 ± 4.16	-0.16 ± 0.28
1984–2002	9.8	-6.72 ± 2.78	-0.34 ± 0.16
2002–2007	10.0	-3.95 ± 2.33	-0.71 ± 0.42
1984–2007	9.8	-13.00 ± 2.84	-0.53 ± 0.15

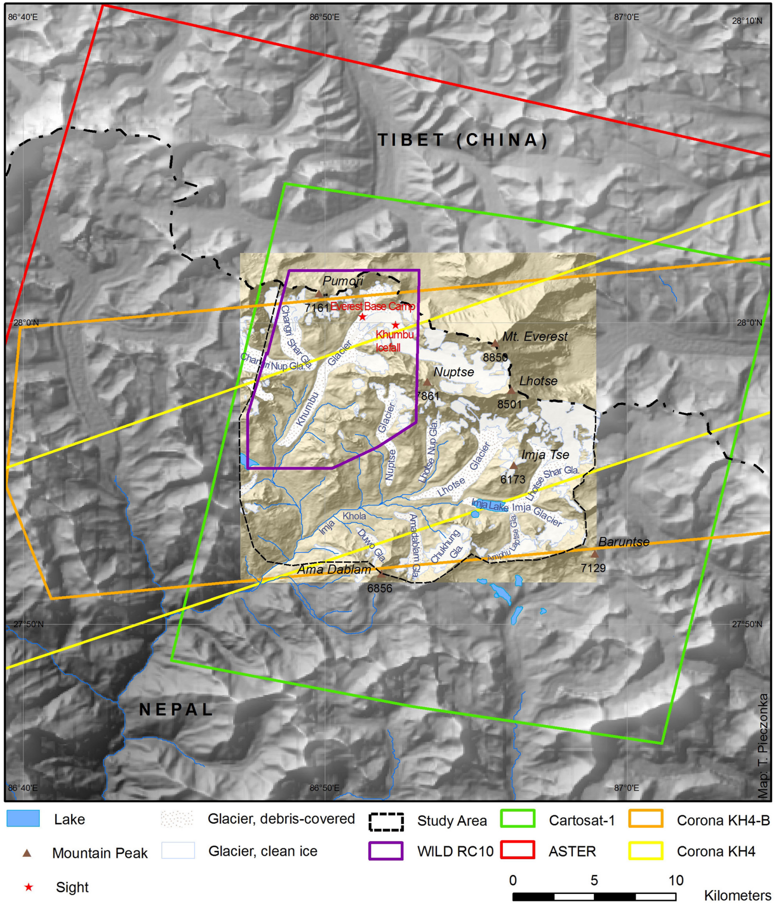

Fig. 1. Study area; location, names and debris-covered portion of the glaciers in the study area, and coverage of the utilized satellite data. Background: SRTM3 CGIAR, Vers. 4, study area: ASTER DTM; glacier outlines based on Bolch et al. (2008b).

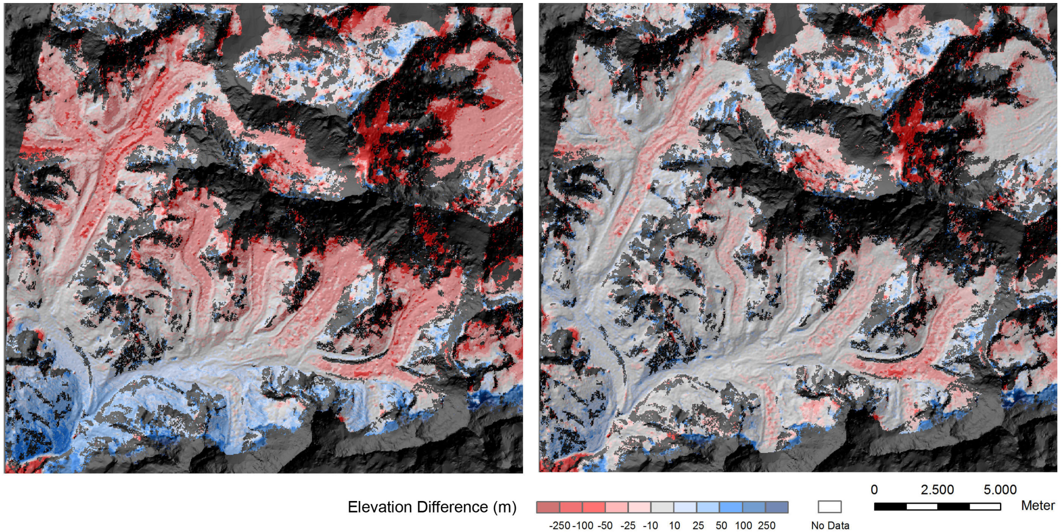

Fig. 2. Elevation difference of 1970 Corona and 2007 Cartosat DTM before (left) and after adjustment (right).

TCD
4, 2593–2613, 2010

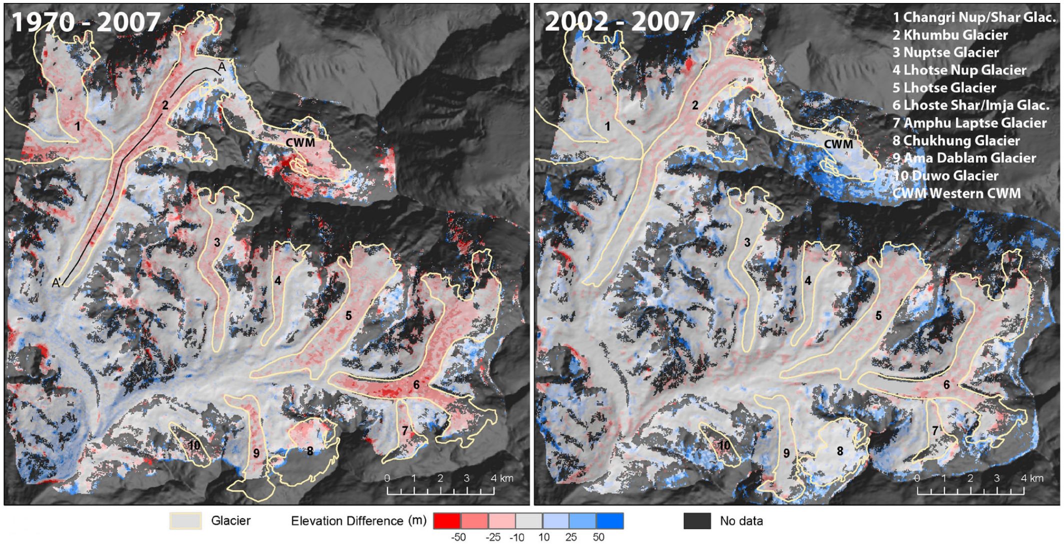

Fig. 3. DTM differences of the study area 1970–2007 and 2002–2007.

TCD
4, 2593–2613, 2010

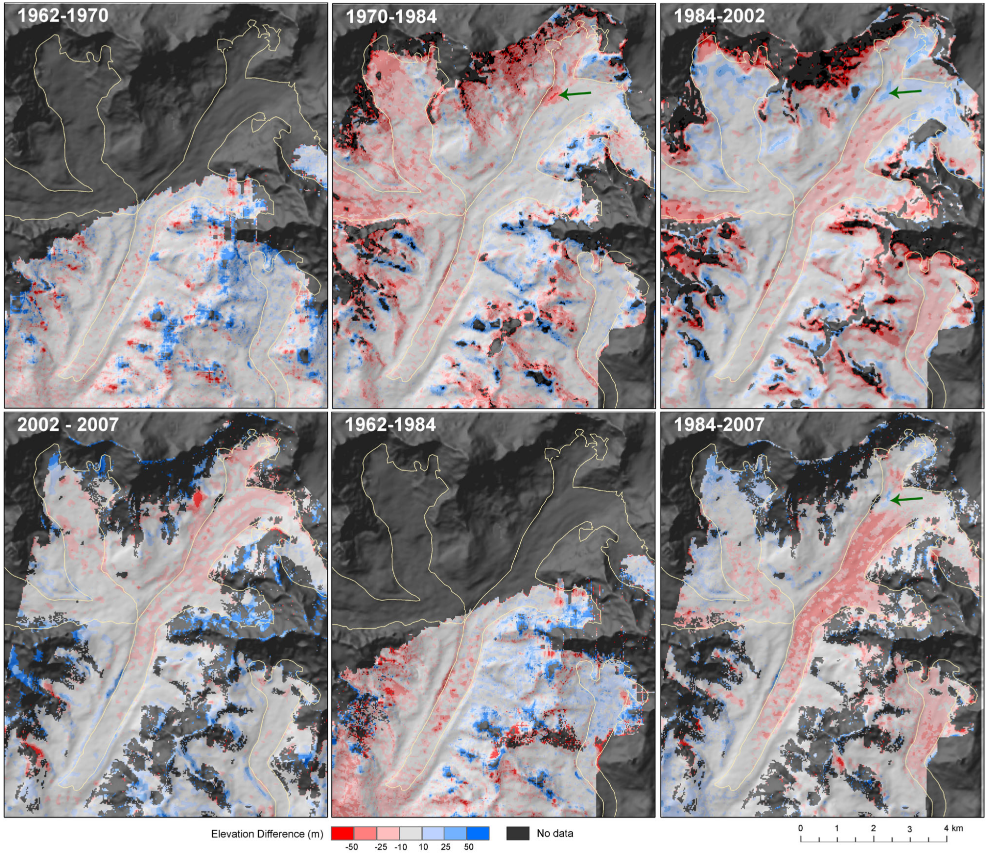

Fig. 4. DTM differences on Khumbu Glacier for different times.

TCD
4, 2593–2613, 2010

Himalayan glacier mass changes

T. Bolch et al.

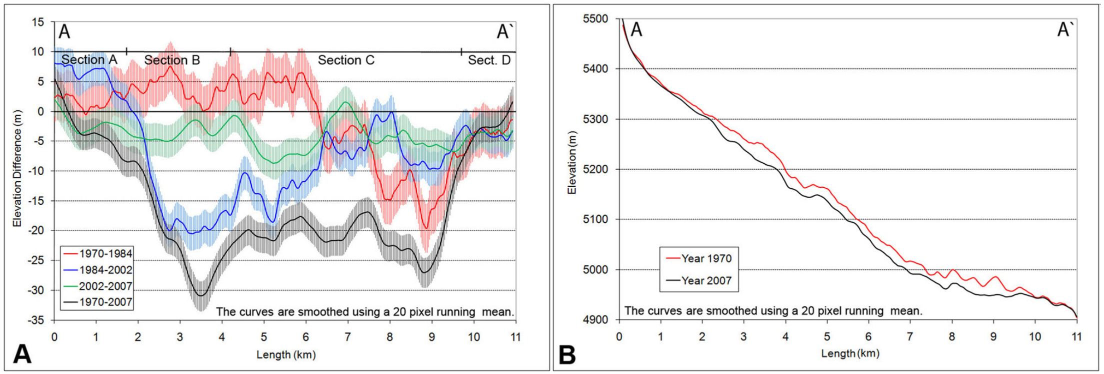

Fig. 5. (A) Profiles of the DTM differences of Khumbu Glacier. **(B)** Longitudinal profiles of the surface elevation of Khumbu Glacier 1970 and 2007. See Fig. 3 for the location of the profiles.

TCD
4, 2593–2613, 2010

Himalayan glacier mass changes

T. Bolch et al.